Colloids and Surfaces A: Physicochemical and Engineering Aspects (2011). 382(1-3), 118-123.
DOI: http://dx.doi.org/10.1016/j.colsurfa.2010.12.005

The use of dolomite as foaming agent and its effect on the microstructure of aluminium metal foams—Comparison to titanium hydride

D.P. Papadopoulos [a], H. Omar[a], F. Stergioudi [a], S.A. Tsipas [b], N. Michailidis [a,*]

[a] Department of Mechanical Engineering, Physical Metallurgy Laboratory, Aristotle University of Thessaloniki, GR 54124 Thessaloniki, Greece
[b] Dpto. Ciencia e Ingenieria de Materiales e Ingenieria Quimica, Escuela Politecnica Superior, Universidad Carlos III de Madrid, Avda de la Universidad 30, 28911 Leganes, Spain

Abstract: In this paper dolomite $MgCa(CO_3)_2$ a naturally occurring mineral was demonstrated to be an effective foaming and stabilizing agent for aluminium with several notable advantages relative to the currently used titanium hydride foaming agent. Characteristic cell structures and microstructural features of foams produced with a dolomite foaming agent are examined and the properties of dolomite based foams produced in a one step process are compared with those produced using titanium hydride based process. The most notable structural feature of dolomite based foams is a smaller cell size and thinner cell faces. Foaming with $MgCa(CO_3)_2$ also gives rise to a marked increase in the stability of molten foams with a large range of foaming temperatures possible, and an almost complete absence of melt drainage even with extended foaming times. Many of these properties are attributed to the cell surfaces being covered by a thin oxide film formed during the foaming process.

Keywords: Metal foam, Dolomite, Microestructre, Characterization

1. Introduction

Metal foams are structural materials in which gas bubbles are separated by thin metal walls and they exhibit a unique combination of properties mainly derived from their cellular structure. These materials have received great attention over the last few years, and they show a great potential for a wide range of industrial applications. Many methods have been used to produce foams [1]. A widely used procedure for Al is melt foaming. This method involves the addition of agents to the molten metal. These agents are added in order to increase either melt viscosity, or to produce gas bubbles, which are trapped into the liquid metal thus producing metal foam. Direct foaming methods of metal melts produce irregular cell structures and inhomogeneous cell sizes, so it is necessary to increase the viscosity of metal melts in order to prevent gas bubble from escaping and coalescing. Additions of ceramic particles such as SiC, MnO_2 and Al_2O_3 to metal melts, is a good approach for increasing viscosity and stabilizing the cell wall [2–4]. It should be noted that the effect of the these added particles is reported primary in the context of stabilization of the foam through the wetting process and particle interaction phenomena such as the development of capillary and interfacial forces and secondly as a mechanism of drainage retardation [5,6]. In liquid metallurgy the most commonly employed foaming agent for aluminium alloys is titanium hydride (TiH_2). It is used mainly because of its high specific hydrogen content, a reasonably good correspondence between its decomposition temperature and typical Al alloys melting temperatures and the rapid kinetics of the decomposition reaction [7–12].

The recently developed dolomite based foaming process [13] suitable for the melt route production, eliminates the problem of premature gas release during the powder dispersion in the melt and has been demonstrated that dolomite can be an efficient foaming agent for producing acceptable quality of closed cell Al foams in a one step process and at a very low cost. Additionally improved performance of dolomite-based foams relies on formation of stabilizing MgO phases [14]. In the current paper the performance of dolomite as foaming and stabilizing agent is studied in detailed and the associated Al-melt foaming behaviour is discussed, compared with the titanium hydride addition.

2. Experimental procedures

2.1. Material production

Titanium hydride based metal foams were produced by the melt foaming procedure. Initially Ca (1.8 wt.%), mean particle size of about 1190 μm supplied by Aldrich Chemical Company was dispersed in molten Al (commercial Al composition: 99.8 wt.% Al and 0.15 wt.% Fe) at 720 °C in order to increase the melt viscosity and the melt was stirred at a speed of 700 rpm for 8 min. TiH_2 powder (1.5–2 wt.%), with a mean particle size of about 44 μm was then introduced at 680 °C into melt and the melt was stirred at a speed

Table 1
Density, relative density and porosity of the metal foams specimens.

Material	Foaming agent (wt.%)		Density of the foam (g/cm^3)	Relative density of the foam (ρ^*/ρ_s)	Porosity (%)
A1	$MgCa(CO_3)_2$	1.5	0.467	0.173	82.7
A2		3	0.773	0.286	71.4
A3	TiH_2	1.5	0.625	0.231	70.03
A4		2	0.571	0.22	68.9

of 1200 rpm for 10 min in order to obtain uniform powder distribution. The melt was kept in the furnace for 3 min to allow the hydride to undergo thermal decomposition and the gas generated in the melt to produce foaming. Finally the foam was allowed to solidify by removing the melt container from the furnace and allowed to cool in air.

The raw material for preparing dolomite based foams was molten Al (commercial Al composition: 99.8 wt.% Al and 0.15 wt.% Fe) and $MgCa(CO_3)_2$ powder. Dolomite powder (1.5–3 wt.%) was introduced at 650 °C into melt and the melt was stirred at a speed of 1200 rpm for 90 s in order to obtain uniform powder distribution. The melt was kept in the furnace for 13 min to allow the dolomite to undergo thermal decomposition and the CO_2 gas generated in the melt to produce foaming.

The thermal history of the foams heating profile was recorded using a K-type thermocouple located directly in the melt. The apparatus used for both (hydride and dolomite) foaming processes mainly consists of a resistance furnace and a stirring paddle driven by a motor which can provide various stirring speeds.

2.2. Material characterization

Particle size distribution of the dolomite used, was measured using a Malvern MasterSizer 2000 Ver. 5.40. Thermogravimetric analysis was used to study the effect of foaming agent type on the onset temperature and kinetics gas evolution. The experiments were carried out in a Setaram Setsys 16/18 TG-DTA analyzer. The amount of analyzed particulate was 20 mg and the samples were heated to 1000 °C at a heating rate of 20 °C min^{-1}.

All the metal foams samples were sectioned by diamond cutting machining in order to minimize local cell wall damage. Also the specimens were ground with a series of SiC papers and afterwards further polished with 1 μm alumina solution. The metal foam structure was examined by light optical microscopy (LOM) for examination of the ceramic particle distribution in the cross-sections of the foam cell faces and scanning electron microscopy (SEM) for microstructural and chemical analysis of the foam sections and foaming agents. The LOM unit was a Leica™ and a digital camera DFC 290. To measure the cell wall thickness, a QManuallA V3.2 image analysis system was used. The SEM unit used was a JEOL model JSM-5900LV. Some of the pore surfaces were also examined after etching with Keller (HF1%) solution. The density of the specimens was determined using a simple volumetric technique, weighting the sample and measuring their external dimensions.

Samples of the dolomite metal foams were prepared for analysis by X-ray powder diffraction using Philips PW 1050 unit.

3. Results and discussion

3.1. Relative density

The average relative densities of the metal foams investigated are shown in Table 1, where ρ^* is the density of the foam and ρ_s the density of aluminium. It can be seen that for the same amount of foaming agent, dolomite based metal foams exhibit higher porosity levels.

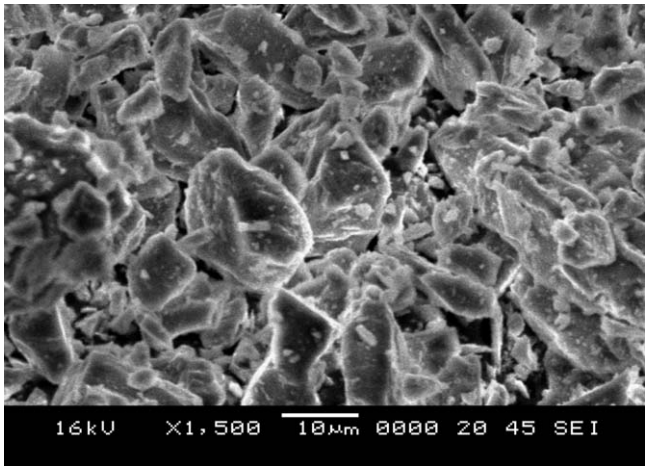

Fig. 1. SEM micrograph of powder dolomite foaming agent used in a current study.

3.2. Gas evolution kinetics

In order to assess the effect of purity and particle size on the kinetics of foaming, dolomite powder was analyzed. A SEM micrograph of dolomite powder is shown in Fig. 1. The natural dolomite fine powder had a slightly white color, the measured distribution of powder size is shown in Fig. 2. The average particle size found ~46 μm.

X-ray powder diffraction pattern obtained for the dolomite powder is shown Fig. 3. The powder is composed of pure dolomite and noticeable amounts of impurities were not detected.

In order to determine a reasonable foaming temperature of the melt, the decomposition temperature of $MgCa(CO_3)_2$ foaming agent was determined using thermogravimetric analysis (Fig. 4). According to the thermogravimetric analysis curves of dolomite, the starting temperature for CO_2 evolution is around 630 °C. Actually the thermal decomposition of powdered samples is strongly influenced by the rate of removal of CO_2 which is in turn dependent on the particle size and packing efficiency of the powder, the gas removal and the sample size [13].

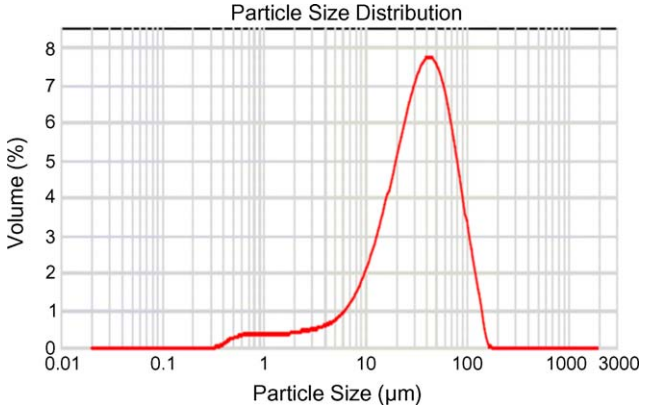

Fig. 2. Measured size distribution of the dolomite foaming agent used for precursor.

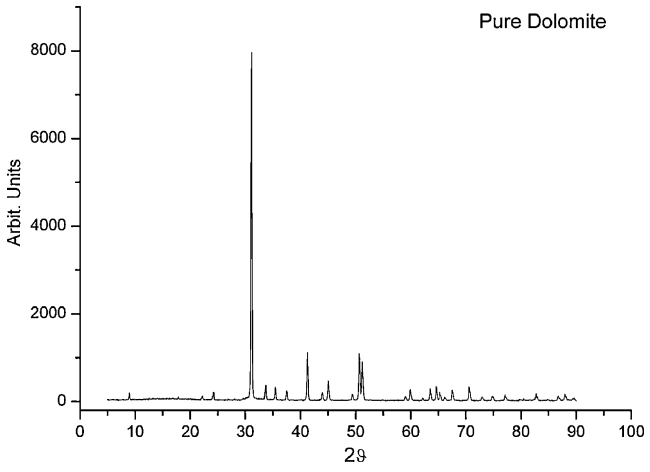

Fig. 3. X-ray diffraction patterns using Cu Kα radiation obtained for the dolomite powder used for the produced Al closed-cell foams.

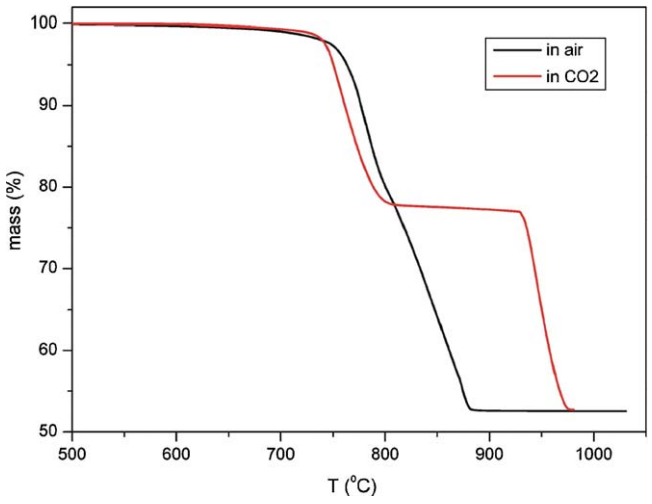

Fig. 4. Thermogravimetric analysis curves of dolomite powder. These experiments were carried out in CO_2 (red curve) or in air (black curve) atmosphere. The heating rate was 20 °C min^{-1}. (For interpretation of the references to color in this figure legend, the reader is referred to the web version of the article.)

On the other hand the direct decomposition of TiH_2 in an atmosphere of hydrogen gas occurs at ~490 °C. In practice foaming with TiH_2 takes place rapidly at lower temperature and TiAl and $TiAl_3$ intermetallics have been observed [15] at the interface between titanium hydride and the metal matrix suggesting parallel reactions taken place. The above characteristics show that the onset temperature of CO_2 evolution from dolomite powder is higher compared to that of hydrogen from titanium hydride.

3.3. Cell morphology

It was apparent from the macrostructures of the produced foams that the pore size and cell wall thickness of the dolomite based foams is significantly smaller than that of the hydride based foams, despite the fact that the baking time for the former foams was about 13 min while for the later was only for 3 min. A cross sectional cell structure of typical dolomite and hydride metal foams is shown in Fig. 5. The overriding difference between the foams is the consistently smaller cell size obtained in the dolomite based process. Apart from the difference in scale all the specimens have similar polyhedral cell structures, with straight or gently curved cell faces and apparently smooth cell surfaces.

Voids up to an order of magnitude larger than the surrounding cells are occasionally visible as well as abnormally large pores. Corresponding statistical measures of a pore size distribution in typical dolomite and hydride based foam of comparable ρ^*/ρ_s are shown in Fig. 6.

There is a significant difference in cell size between the centre and the edges of the foams. The marked drainage in the hydride based foams compares with an almost negligible rate of drainage in the dolomite based foams. The low rate of drainage is partly a result of the smaller cell size in dolomite based foams. Additionally cell coalescence in the hydride based foams is associated with rapid rejection of melt from cell faces to plateau borders and force melt flow and redistribution. The stability of ruptured cell faces in dolomite based metal foams means that the faces remain narrow with a strong influence of surface viscosity and complete absence of forced melt flow redistribution. The cell size in hydride based metal foam increased by a factor of approximately 2 at the centre of the specimens, with not marked increase in cell size at the top of the foam. Gravity drainage is a common reason for both types of foams, giving rise to density gradients along the structure.

Examination of polished cross sections demonstrates that the surface concentration of unreacted dolomite particles is with the largest face of the particles generally aligned almost parallel to the surface. As shown in Fig. 7 although dolomite particles are close to the surface, a continuous film of Al matrix is invariably present at the interface.

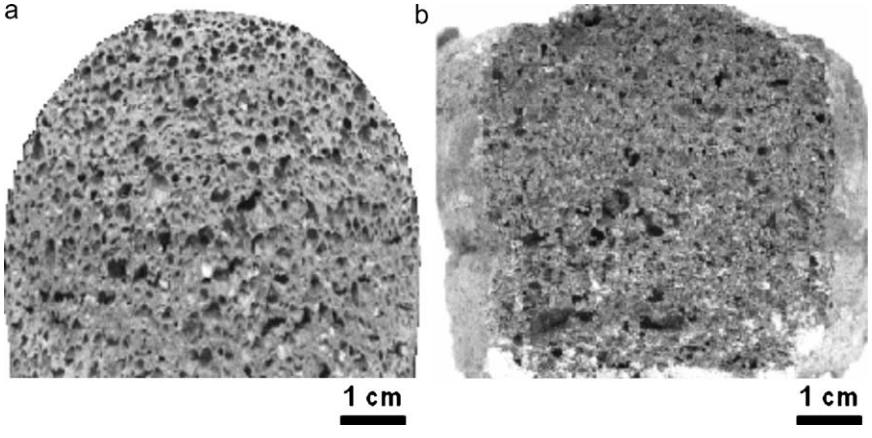

Fig. 5. Typical cross sectional cell structures of hydride- and dolomite-based foams: (a) foam produced by foaming a foamable precursor with 1.8 wt.% TiH_2 particles, T_{foam} = 720 °C, t_{foam} = 3 min, ρ^* = 0.569 g/cm^3 and ρ^*/ρ_s = 0.219. (b) Foam produced by foaming a foamable precursor with 2 wt.% $MgCa(CO_3)_2$, T_{foam} = 720 °C, t_{foam} = 13 min, ρ^* = 0.773 g/cm^3 and ρ^*/ρ_s = 0.286.

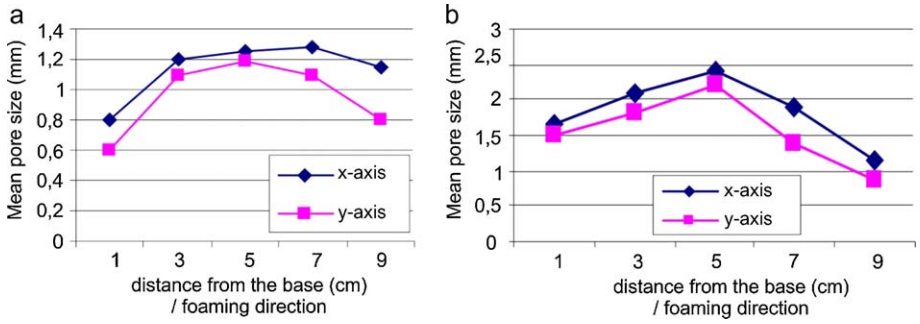

Fig. 6. Distribution of pore size along the *X* and *Y* axis of: (a) dolomite based foam containing 3 wt.% dolomite, produced with T_{foam} = 650 °C, t_{foam} = 13 min, ρ^* = 0.705 g/cm^3 and ρ^*/ρ_s = 0.261. (b) Hydride based foam containing 1.8 wt.% Ca, 1.4 TiH_2, produced with T_{foam} = 720 °C, t_{foam} = 3 min, ρ^* = 0.713 g/cm^3 and ρ^*/ρ_s = 0.264.

Dolomite particles have been reported [16] to become gradually more wettable in pure aluminium due to the formation of interfacial Al_4C_3. Al_4C_3 forming reactions do not appear to be significant in our process as no Al_4C_3 has been detected in the current work using XRD. The absence of aluminium carbide is consistent with the slow kinetic formation reported in the literature [16]. The macroscopic similarity of the cell structure of hydride and dolomite metal foams is remarkable in view of the marked difference in the distribution of nominally surfactant particles. In the thinnest cell walls the bridging particles apparently hold the two faces apart giving rise to bumps on the surface of thinner cell faces. The limiting face thickness is thus related to the dimensions of the refractory particles.

In dolomite based foams, particles were uniformly distributed throughout the foam (Fig. 8). This high concentration is attributed to relatively free drainage of the Al melt through the relatively wide plateau borders and cell faces, while the dolomite particles remains attached to the surfaces of the cells or constrained by loose networks of solid particles in the narrow channels.

3.4. Cell microstructure

In titanium hydride based foams the cell walls consist of Al dendrites, as expected after quite slow cooling of an Al melt containing Ca and Ti. Additionally titanium hydride particles were found both on the surface and embedded within cell faces. In the latter case the particles were often surrounded by a visible layer of a Ti–Al compound identified by SEM as $TiAl_3$ (Fig. 9). According to the literature [15] the later is the expected product when TiH_2 reacts with liquid aluminium to release hydrogen gas and suggesting that the foaming reaction did not take place very efficiently.

On the other hand dolomite particles were never embedded in the matrix and were generally fairly loosely attached to the surface of cells with no discernible reaction with the adjacent metal melt. The presence of several particles per cell is presumably due to incomplete dispersion of the foaming agent evidenced by the presence of several particles present in pores in the foamable precursors. It may also be the result of coalescence of initially separate cells during the foaming process. Fig. 10 suggests that as a result of reaction between CO_2 and the Al melt, a thin solid layer forms during the foaming process, capturing and creating a significant segregation of the unreacted particles along the pores surfaces.

These oxides layers seem to promote the stabilization of the cells against coarsening and coalescence during the foaming process. Diffraction patterns obtained with the main diffraction peaks identified are shown in Fig. 11. The diffractions patterns are dominated by Al peaks confirming the formation of Al grains in three crystallographic layers (◊1,◊2,◊3) and the concentration of oxides such as MgO (Δ), Al_2O_3 (●), $CaMg(CO_3)_2$ (▲) but in a very low amount.

The fact that the phase of Ca or CaO does not appear in the XRD diagram as it should be expected taking into account the raw materials is consistent with other reports [15]. The later is due to the coefficient of mass absorption which is very high for calcium (Ca = 142) and less for magnesium (Mg = 38,6). As illustrated in Fig. 12 the cell walls chemical analysis revealed a presence a network of Mg–Ca–Al–O elements which corresponds to a ternary system of $CaO–Al_2O_3–MgO$ oxides or unreacted dolomite particles.

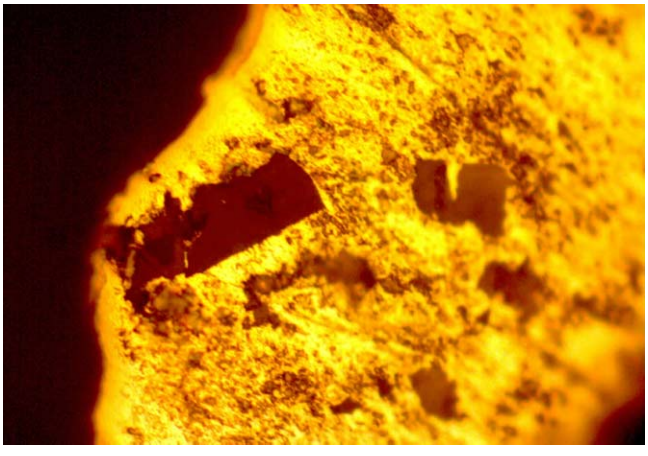

Fig. 7. Optical micrograph showing cross section of thin cell face of dolomite based foam. The surface segregation of the unreacted non-equiaxed dolomite particles (dark brown) is prominent (50×). (For interpretation of the references to color in this figure legend, the reader is referred to the web version of the article.)

Fig. 8. Optical micrograph of a cell wall in a dolomite based foam produced with T_{foam} = 650 °C, t_{foam} = 13 min, ρ^* = 0.705 g/cm^3 and ρ^*/ρ_s = 0.261 (50×).

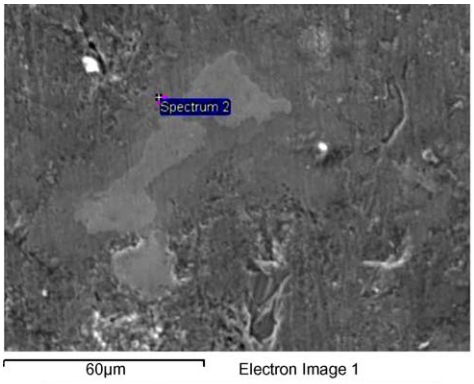

Element	Ti	Al	Totals
Weight%	92.98	07.02	100.00
Atomic%	87.85	12.15	100.00

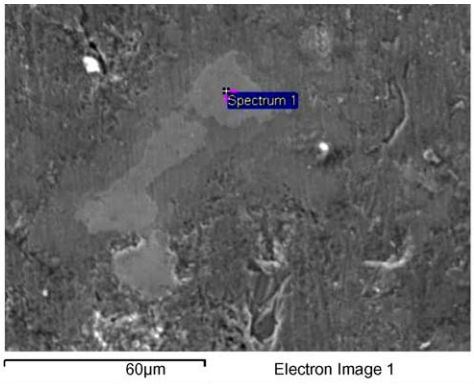

Element	O	Ti	Ca	Al
Weight%	05.08	12.87	05.82	76.22
Atomic%	08.93	07.56	04.09	79.43

Fig. 9. SEM micrographs and chemical analysis of cell wall hydride based foam by foaming a foamable precursor with 1.8 wt.% TiH_2 particles, $T_{foam} = 720\,^{\circ}C$, $t_{foam} = 3$ min, $\rho^* = 0.569\,g/cm^3$ and $\rho^*/\rho_s = 0.219$.

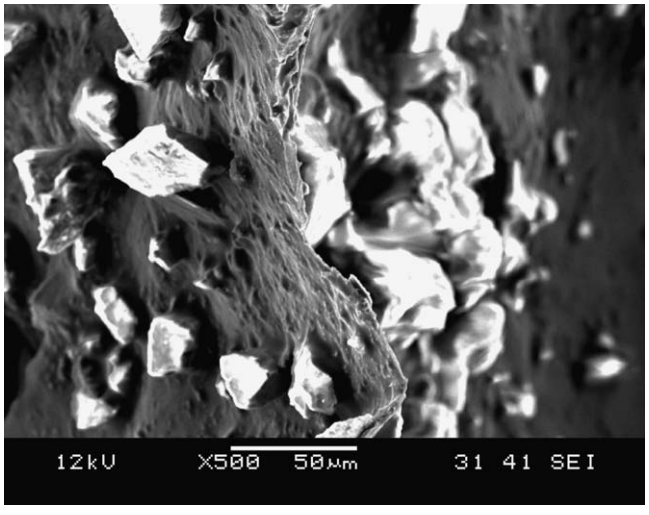

Fig. 10. SEM micrograph of the cell surfaces in dolomite based foam showing several surface attached particles of the foaming agent along the solid skin of the pores.

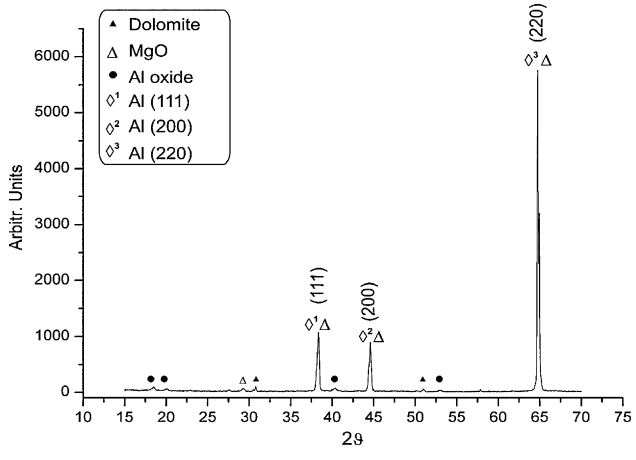

Fig. 11. X-ray diffractions traces using Cu Kα radiation obtained a dolomite based foam produced with $T_{foam} = 650\,^{\circ}C$, $t_{foam} = 13$ min, $\rho^* = 0.705\,g/cm^3$ and $\rho^*/\rho_s = 0.261$.

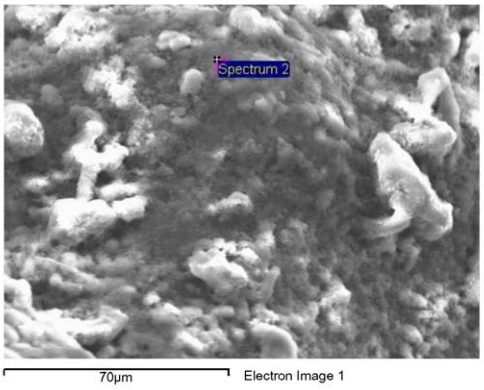

Element	O	Mg	Al	Ca
Weight	59.66	0.58	39.05	0.70
Atomic	71.47	0.46	27.74	0.34

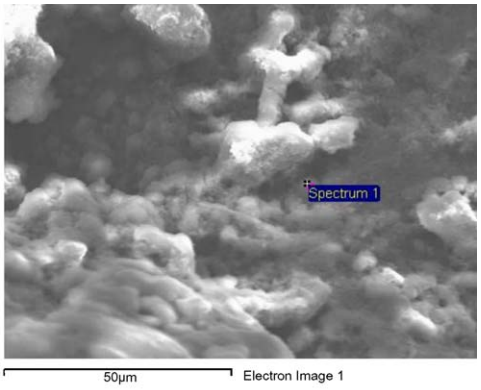

Element	O	Mg	Al
Weight	56.47	0.41	42.55
Atomic	68.70	0.33	30.69

Fig. 12. SEM micrograph of the cell surfaces in dolomite based foam showing several surface attached particles of the foaming agent.

4. Conclusions

The use of TiH_2 as a foaming agent for aluminium foam production involves high cost of the raw material and hazards due to the nature of specific fine powder. Careful process control is required to obtain reproducible cell structures with a strong sensitivity to fluctuations in foaming temperature and a risk of heating. Titanium hydride based foams had smooth surface walls with no visible particles attached. On the other hand the chemical decomposition of dolomite is more gradual at the temperature of aluminium melts. Dolomite acts both as foaming and stabilizer agent by a decomposition reaction at elevated temperatures and by the release of carbon dioxide gas. The reaction of CO_2 with the liquid aluminium leads to the formation of thin films of solid oxides and raises the mechanical stability of cells [13]. The reduced rate of foaming also improves control over the foaming process, while the low material cost and non hazardous nature are also favourable.

References

[1] J. Banhart, Manufacture, characterization and application of cellular metals and metal foams, Prog. Mater. Sci. 46 (2001) 559–632.
[2] S.W. Ip, Y. Wang, J. Toguri, Aluminum foam stabilization by solid particles, Can. Metall. Quart. 38 (1999) 81–92.
[3] C. Korner, M. Arnold, R.F. Singer, Metal foam stabilization by oxide network particles, Mater. Sci. Eng. A-Struct. 396 (2005) 28–40.
[4] S. Esmaeelzadeh, A. Simchianal, D. Lehmbus, Effect of ceramic particle addition on the foaming behaviour, cell structure and mechanical properties of P/M AlSi7 foams, Mater. Sci. Eng. A-Struct. 424 (2006) 290–299.
[5] C. Körner, Foam formation mechanisms in particle suspensions applied to metal foams, Mater. Sci. Eng. A-Struct. 495 (2008) 227–235.
[6] G. Kaptay, On the equation of the maximum capillary pressure induced by solid particles to stabilize emulsions and foams and on the emulsion stability diagrams, Colloid Surf. A-Physicochem. Eng. Aspects 282–283 (2006) 387–401.
[7] J.C. Elliot, US Patent 2,983,597 (1961).
[8] V. Gergely, H.P. Degischer, T.W. Clyne, Compr. Compos. Mater. (2003) 797–820 (Chapter 3.30).
[9] A.E. Simone, L.J. Gibson, The effects of cell face curvature and corrugations on the stiffness and strength of metallic foams, Acta Mater. 46 (1998) 3929–3935.
[10] J. Frei, V. Gergely, A. Mortensen, T.W. Clyne, The effect of prior deformation on the foaming behaviour of FORMGRIP precursor material, Adv. Eng. Mater. 4 (2002) 749–752.
[11] L. Ma, Z. Song, Cellular structure control of aluminium foams during foaming process of aluminium melt, Scripta Mater. 39 (1998) 1523–1528.
[12] V. Gergely, H.P. Degischer, T.W. Clyne, Recycling of MMCs and Production of Metallic Foams in Comprehensive Composite Materials, 2003, pp. 797–820.
[13] D.P. Papadopoulos, PhD Thesis, Aristotle University of Thessaloniki, Department of Mechanical Engineering, 2008.
[14] M. Haesche, D. Lehmhus, J. Weise, M. Wichmann, I.C.M. Mocellin, Carbonates as foaming agent in chip-based aluminium foam precursor, J. Mater. Sci. Technol. 26 (2010) 845–850.
[15] A. Markaki, T. Clyne, The effect of cell wall microstructure on the deformation and fracture of aluminium-based foams, Acta Mater. 49 (2001) 1677–1686.
[16] S.M. Oak, B.J. Kim, W.T. Kim, M.S. Chun, Y.H. Moon, Physical modeling of bubble generation in foamed-aluminum, J. Mater. Process. Technol. 6302 (2002) 1–6.